LBL-11874 .2
Preprint

Lawrence Berkeley Laboratory
UNIVERSITY OF CALIFORNIA

CHEMICAL BIODYNAMICS DIVISION

Submitted to the Journal of the American Chemical Society

THE STATE OF MANGANESE IN THE PHOTOSYNTHETIC APPARATUS. I. EXAFS STUDIES ON CHLOROPLASTS AND di-μ-oxo BRIDGED di-MANGANESE MODEL COMPOUNDS

J.A. Kirby, A.S. Robertson, J.P. Smith, A.C. Thompson, S.R. Cooper, and M.P. Klein

November 1980

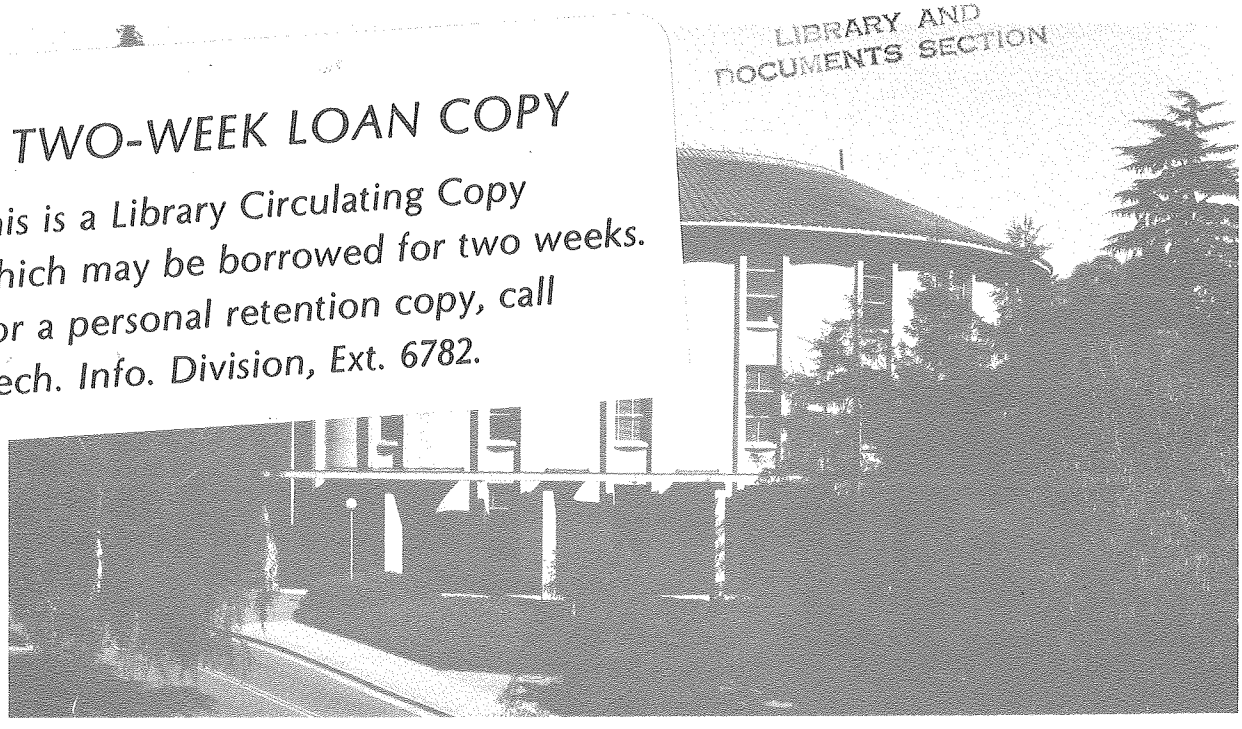

Prepared for the U.S. Department of Energy under Contract W-7405-ENG-48

DISCLAIMER

The State of Manganese in the Photosynthetic Apparatus. I.

EXAFS Studies on Chloroplasts and di-μ-oxo Bridged di-Manganese Model Compounds

J. A. Kirby*,++, A. S. Robertson**, J. P. Smith+, A. C. Thompson, S. R. Cooper++, and M. P. Klein

Laboratory of Chemical Biodynamics, Lawrence Berkeley Laboratory, University of California, Berkeley, CA 94720

*Current address: TRW, Inc., One Space Park, Redondo Beach, CA 90278

**Current address: Shell Oil Company, One Shell Plaza, Houston TX 77001

+Current address: Chemistry Division, Argonne National Laboratory, Argonne, IL 60439

++Current address: Department of Chemistry, Harvard University, Cambridge, MA 02138

Reprint requests

ABSTRACT: Extended X-ray Absorption Fine Structure (EXAFS) studies on the manganese contained in spinach chloroplasts and on certain di-u-oxo bridged manganese dimers of the form $(X_2Mn)O_2(MnX_2)$ (X = 2,2'-bypyridine and 1,10-phenanthroline) are reported. From these studies, the manganese associated with photosynthetic oxygen evolution is suggested to occur as a bridged transition metal dimer with most likely another manganese. Extensive details on the analysis are included.

INTRODUCTION

Since the original observation in 1937 by Pirson[1] of an absolute requirement in photosynthesis for the trace element Manganese, the specific role that Mn plays has been a subject of extensive research. The general consensus is that the Mn is directly involved in photosyntehtic oxygen evolution either at the active site or as a critical component of the electron transport chain (see review by Radmer and Cheniae[2] for further details). Until now all observations which have been made concerning the activity of the chloroplast bound Mn have been by indirect methods such as NMR water proton relaxation experiments[3] and Mn release experiments using some chemical[4] or physical[5] treatments. The experimental work reported in this paper and its companion[6] is the first direct observation of the Mn contained in chloroplasts. The technique used was X-ray Absorption Spectroscopy (XAS) utilizing the tunable X-ray sources at the Stanford Synchrotron Radiation Laboratory (SSRL), Stanford, CA.

Two types of information can be obtained from XAS. The first is an estimate of the formal oxidation state of the element of interest using X-ray Absorption Edge Spectroscopy. Such studies on the Mn in chloroplasts are reported in the accompanying paper.[6] The other information allows the

determination of the local structure around the atom whose XAS spectrum is being obtained. This type of experiment utilizes the post-absorption edge modulations of the photoelectron cross section which is known as Extended X-ray Absorption Fine Structure (EXAFS). The theoretical basis of the effect has been well established by Stern and by Ashley and Donaich in references 7 and 8 respectively. Analysis of the modulation patterns yield the radial distances to the neighboring atoms. To some extent the backscattering probabilities can be used for elemental identification of the ligating atoms.[9,10]

It has been known for many years that there are at least two different classes of Mn in chloroplasts. The larger fraction, the "loosely bound pool", is known to be essential for O_2 evolution. This "loosely bound pool" represents approximately 2/3 of the total Mn and the release from its normal site into an aqueous phase can be accomplished by physical and chemical methods.[2] In order to differentiate between these two clases of Mn, X-ray spectra were collected on chloroplasts capable of oxygen production ("active" chloroplasts) and on chloroplasts which had the "loosely bound pool" of Mn completely removed and thus were incapable of oxygen evolution ("inactive" chloroplasts).

MATERIALS AND METHODS

The preparation of various chloroplast samples is detailed in the companion paper[6,23] and will not be repeated here. The two samples used were an "active" broken chloroplast pellet and an "inactive" chloroplast pellet which had the "loosely bound pool" of Mn removed by treatment with Tris buffer (Tris = alkaline Tris-(hydroxymethyl)aminomethane) followed by osmotic shock. Complete removal of all aqueous Mn^{+2} was monitored by measurements of the Mn^{+2} EPR signal.

A number of model compounds were prepared or purchased for comparison with the chloroplast samples. The three reported here, di-μ-oxo-tetrakis-(2,2'-bipyridine) dimanganese (III,IV) perchlorate, Mn(3,4)Bipy, di-μ-oxo-tetrakis(1,10-phenanthroline) dimanganese (III,IV) perchlorate Mn(3,4)Phen, and di-μ-oxo-tetrakis(1,10-phenantroline) dimanganese (IV,IV) perchlorate Mn(4,4)Phen, were prepared and characterized by literature methods.[11,12,13] The powdered crystalline samples were mixed with a binding agent of powdered cellulose and pressed into 1-1/4 inch diameter pellets in sufficient quantities so that approximately 90% of the incident X-ray flux was absorbed in the sample when the X-ray energy was just higher than the Mn K or 1s absorption edge.

EXPERIMENTAL

The X-ray absorption spectra were obtained at the Stanford Synchrotron Radiation Laboratory (SSRL). The model compound data were collected in the standard absorption mode, described elsewhere.[14] Due to the very low concentration of Mn in the chloroplast samples (of the order of 100 M) and the large background absorption by the rest of the sample (e.g. water, protein, and phospholipid) it was not possible to collect usable absorption

data in a reasonable period of time. The chloroplasts spectra were, instead, collected in the fluorescent detection mode where the relative X-ray absorbance was obtained by measuring the excitation function for X-ray fluorescence characteristic of Mn.[16] The X-ray detector used was a triplet Si(Li) solid state detector built by the Nuclear Instrument and Methods Group at Lawrence Berkeley Laboratory.[17] Even with the sensitivity enhancement provided by the fluorescent EXAFS technique[16], it was still necessary to use the focused X-ray line[15] at SSRL to obtain as intense an incident X-ray flux as possible. The "active" chloroplast spectra were obtained in approximately 24 hours on a focussed line. The inactive chloroplast spectra were obtained in approximately the same amount of beam time two weeks later. The large number of individual spectra were eventually co-added to produce one data analysis spectrum for each sample.

General Data Analysis Method. EXAFS data processing is described in detail elsewhere[18] and thus will be only briefly outlined here.

The first step was to condense the numerous individual spectra that were collected on each sample into one final co-added spectrum. A significant problem at this step was to maintain an energy reference for each spectrum relative to a pre-selected standard. For the chloroplast spectra this presented some problems which are addressed later. The data are then expressed as a relative EXAFS modulation, generally defined by[7,8]

$$\chi(k) = [\mu(k) - \mu_{BG}(k)]/\mu_0(k) \qquad (1)$$

where χ is the fine structure modulation (EXAFS), μ is the observed X-ray absorption cross section, μ_0 is the photoelectric cross section for the free atom, and μ_{BG} is the experimentally derived background which in the absence

of experimental baseline would be the free atom photoelectric cross section μ_0. As indicated in Equation 1, the EXAFS modulation, χ, is not expressed as a function of the incident X-ray photon energy but as a function of the resultant photoelectron wave vector defined by

$$k = 2\pi(2m_e(E-E_0))^{1/2}/h \qquad (2)$$

where k is the photoelectron wavevector in Angstroms^{-1}, E is the energy of the incident photon in eV, E_0 is the K-shell binding energy in eV, m_e is the mass of the electron and h is Planck's constant.

To obtain $\chi(k)$ from an X-ray spectrum, a number of procedures are utilized. First, a preabsorption edge background is removed from the spectrum. Then the spectrum is divided by the free atom photoelectric cross section (Victoreen formula) and a low frequency background is removed. Since only relative absorption cross sections are treated, it is necessary to normalize the spectrum to obtain an edge height of one. In the final operation, the energy spectrum is expressed as a function of photoelectron wave vector space, hereinafter called k-space. In order to make this conversion it is necessary to choose a value for the binding energy, E_0 for the excited K-electron. At the present time there is no reasonable a priori method for estimating E_0 so approximate values are used for the first iteration.

The next analysis step is to examine the power spectra of the fourier transforms of $\chi(k)$ multiplied by different powers of k(k^n (k)) As can be seem from the theoretical form for $\chi(k)$[7,8]

$$\chi(k) = \sum_{i=1}^{n_s} \frac{N_i}{kR_i^2} e^{+\sigma_i k^2} |f_i(k,\pi)| \sin(2kR_i + \alpha_i(k)) \qquad (3)$$

(where n_s = number of scattering shells N_i = number of atoms in the i^{th} shell, R_i = distance to the i^{th} shell in Angstroms (Å), $f_i(k,\pi)$ = backscattering amplitude for the i^{th} shell, σ_i = disorder parameter for the i^{th} shell, and $\alpha_i(k)$ = scattering phase shift). The Fourier transform of the k-space data yields a radial distribution function of the neighboring atoms hereafter called R-space. However, the Fourier transforms give only approximate distances and tentative elemental identifications, due to nonlinearities in the phase shift functions $\alpha_i(k)$ and asymmetry of the amplitude functions $f_i(K,\pi)$. More exact determinations are made by curve fitting.

The Teo-Lee model[9] and the Hodgson-Doniach model[19] were used in curve fitting . In the Teo-Lee model, theoretical calculations are used for $f_i(k,\pi)$ and $\alpha_i(k)$ in Equation 3 and the values of N_i, σ_i, R_i and E_{oi} are simultaneously fit.[18] In the H-D model, simple functional forms for $f_i(k,\pi)$ and $\alpha_i(k)$ are assumed and experimental data on model compounds are used to determine them for particular absorber-backscatter pairs.[19]

Each model has its own merits and limitations.[18] In general, the T-L model has the ability to give reasonable fits with highly disordered and chemically altered systems; for certain types of multi-shell fits there are too many parameters. The H-D model, on the other hand, has the advantage of simplicity and fewer fitting parameters (only N_i and R_i); it generally gives unreliable values for the number of scatters and poorer fits.[18] In the following discussion, the H-D fits will be included in the tables of results for comparison, but in general will not be discussed.

Thus, the general analysis procedure is to perform the Fourier transforms and make estimates of the radial distances and guesses for the elements contributing to a given R-space feature. These values and guesses are

then used as the starting points in the curve fitting.

The first curve fits performed are on resolved peaks in the R-space Fourier transforms. These fits are used to make elemental identifications and the first determination of the true radial distance to the atoms represented by the peak. The resolved peak is isolated by applying a window function and this feature is then transformed back to K-space for fitting. A number of single shell fits are performed using the parameters for several reasonable choices of backscattering elements. Using the criteria explained in Reference 18, the elemental identifications and radial distance determinations are made. If two or more R-space peaks are very close together, it is not possible to accurately use the single peak Fourier isolation method. It is then necessary to isolate the composite peak and compute multi-shell fits to make reasonable identification of the ligands involved and their distances. It is often very useful to create simulated data and compare the Fourier transforms and fitting results with the unknown system. The simulated data are essentially equivalent to creating model compounds of known structure. These often aid in identification of complex multi-distance R-space peaks.

The last analysis step is to perform multi-shell fits on a Fourier isolated k-space spectrum which includes all the R-space peaks of interest. This isolation step is only used to remove the residual low frequency background and high frequency noise, thereby greatly improving the precision of the fits.

If a single peak can be isolated, there is one additional method that can be used. With single peaks it is possible to remove the amplitude from the spectrum leaving only a non-linearily phase modulated sine wave. This permits phase-only T-L fits, which often results in better distance

determinations than do total fits.[18] These phase only fits also provide a method of obtaining distance error estimates.[18] All the single shell phase only fits that were performed can be identified in the tables by the presence of error estimates.

RESULTS

Some of the R-space Fourier transform power spectra for the samples studied are presented in Figure 1 and the relative magnitudes and positions for the main peaks are tabulated in Table 2. The representations $k^0\chi(k)$ and $k^3\chi(k)$ indicate that $\chi(k)$ was multiplied by k^0 (=1) and k^3 respectively before the Fourier transform was performed. The purpose in examining the different $k^n\chi(k)$ transforms is to make tentative elemental identifications. With the exception of highly disordered shells, the heavier the element, the higher its relative Fourier transform peak becomes as the power of k^n increases.[18]

di-μ-oxi-bridged Manganese Dimers. The $k^0\chi(k)$ and $k^3\chi(k)$ R-space Fourier transforms for Mn(3,4)Bipy are presented in Figures 1(a) and 1(b) and the crystal structure is presented in Figure 2. The Fourier transforms for the other two model compounds, Mn(3,4)Phen and Mn(4,4)Phen, are quite similar so that comparisons of the distances in Mn(3,4)Phen and Mn(4,4)Phen to the known distances in Mn(3,4)Bipy will be made with curve fits.

The curve fitting results are presented in Table 2. Examination of the contents of Figure 1(a) and 1(b) and of Table 2 leads to three immediate observations. First, the actual error for the average distance for the bridge oxygens (0.007Å) is well within the estimated error (0.019Å) for the T-L model so the comparative results for this shell should be quite

accurate. Second, the Mn shell is about 0.039Å shorter than the crystal structure distance, but all three Mn results are short of the crystallogrpahic result of approximately 2.72Å. This shortening of the Mn-Mn distance seems to be associated with the di-μ-oxo configuration since the only other model compounds examined which had short Mn-Mn distances were Mn_2O_3 and α-M_nO_2 which are also di-μ-oxo bridged. Their distances were short by almost exactly the same amount.[18] Thus all consideration of bridged Mn-Mn distances must take this shortening into account.

The final observation is, perhaps, the most obvious one but at the same time the most perplexing. There is no feature corresponding to the four nitrogens in the first coordination sphere. The large heterogeneity in ligand distances may result in a large interference effect which reduces the nitrogen peak to the noise level. This conclusion was verified by creating a number of different simulations of the oxygen and nitrogen atoms in the first shell of Mn(3,4)Bipy (for an example see Figures 1(i) and 1(j)). The effect will be explained in more detail in the Discussion section.

Chloroplasts. The final co-added spectra for the two chloroplast samples represent approximately 200 seconds of data acquisition per point. The added spectra are presented in Fig. 3.

The reduced counting rate for the "shocked"or inactive chloroplast sample is about that expected if 2/3 of the total Mn is released by the Tris-treatment and removed by the osmotic shock. (The two samples were similar but not identical in chlorophyll concentration and the samples were run under slightly different experimental conditions).

Two other experimental effects should be noted. First, due to the much poorer energy resolution on the focussed line (>10 electron volts (eV)), the added spectra could not be energy referenced to better than a few eV. This

results in a small additional dampening effect on the EXAFS modulations. Second, it should be noted that although the EXAFS data extend to higher photon energies the presence of the iron K-edge at 7100 eV forces truncation of the useable EXAFS data at that energy (see Figure 3(a)).

The first step in analyzing the chloroplast spectra was to examine the Fourier transforms to obtain estimates of ligand distances. By comparison with model compounds and by utilizing the known structural chemistry of Mn, reasonable guesses can be made regarding ligand identity. It should be noted at this point that differentiation between ligands with similar atomic number is not possible with EXAFS at the present time. Therefore, when a reasonable low atomic number ligand of Mn is specified, it will be indicated by CNO representing carbon, nitrogen, oxygen, or some mixture. These elements are all known to ligate Mn and their dominant presence in chloroplasts strongly suggests them as the most likely ligands of low atomic number. In a similar manner, the next heavier elements likely to be encountered in chloroplasts are indicated by PClS (P, Cl, S) and MnFe (note: Cu cannot be excluded when Mn or Fe is indicated).

(a) "Active Chloroplasts. Fourier transform power spectra for $k^0\chi(k)$ and $k^3\chi(k)$ of the "active" chloroplast spectrum of Figure 3(a) are presented in Figures 1(c) and 1(d) and tabulated in Table 1. Examination of Figure 1 and Table 1 leads immediately to a comparison between (a), the first peak in the active chloroplasts and the oxygen shell in Mn(3,4)Bipy (both R_{eff} are approximately 1.3Å in the $k^3\chi(k)$ transforms) and, (b), the third peak of the active chloroplasts and the Mn shell of Mn(3,4)Bipy (both R_{eff} are approximately 2.3Å in the $k^3\chi(k)$ transforms; both grew out of the noise as n in k^n was increased). This similarity is even more striking when the unusual Mn ligand distances represented by these two peaks are compared with

other Mn model compounds.[18] Thus, a good starting point was to assume a CNO first coordination sphere ligand at 1.8Å and a MnFe ligand at 2.7Å, the crystallographic distances for Mn(3,4) Bipy. (see Fig. 2). The fitting analyses problems, however, were complicated by the presence of the second peak in the transform of the active chloroplast. It was too close to the first peak to be isolated so all fits on the first two peaks had to performed on the Fourier isolate of these two peaks together. However, the relatively short distance of the second peak (approximately 2.2Å) and the known chemistry of Mn again suggested CNO ligands.[6,18]

The next step in fitting the active chloroplast spectrum was to examine the isolated third peak in the Fourier transform. Using the criteria developed for elemental identification (positive amplitude at expected distance and comparison of the quality of the fit with different elements),[18,19,21] both fitting models predicted a MnFe atom at an approximate distance of 2.7Å. Due to the high noise level in the spectrum and the lack of a good separation between the peaks, the reported fitting results for this peak are deferred until consideration of the final three shell fits.

The first two peaks were difficult to identify positively. This was finally accomplished by comparing the Fourier isolation of the first two peaks and some of the simulated Mn(3,4)Bipy oxygen-nitrogen first coordination sphere models mentioned earlier. One of the simulations which closely resembled the EXAFS of the active chloroplasts is described in Tables 1 and 3 and its Fourier transforms are presented in Figures 1(i) and 1(j). With this valuable clue it was possible to obtain very good fits to the first two peaks of the active chloroplasts. The isolated spectrum, the simulated spectrum and their best T-L fits are presented in Figure 4. The

one and two shell fitting results for the isolated and the simulated spectra are tabulated in Table 3.

The three shell fits (using two CNO first shells and a Mn third shell as indicated above) are tabulated in Table 4. The noise filtered $k^3(k)$ spectrum and its best T-L fit are presented in Figure 5.

(b) Inactive Chloroplasts. Analysis of the "inactive" chloroplast spectrum was performed with the primary concern of determining the exact extent to which this spectrum, which represents the residual Mn content of chloroplasts after the "loosely bound" Mn was removed, contributes to the "active" chloroplast spectrum. If no evidence of alteration in the state of this "tightly bound" Mn could be found, then an attempt to obtain the (k) spectrum of only the "loosely bound" Mn would be made.

The "inactive" chloroplast Fourier transform power spectra are presented in Figures 1(e) and 1(f) with the peak magnitudes and positions included in Table 1. Examination of the inactive chloroplast transforms shows no apparent correspondence between its first peak and those of any of the active chloroplast peaks. Rather, the peak corresponds to a low valent Mn^{+2} to CNO first coordination sphere distance (approximately 2.1Å when corrected by adding 0.5Å to the $k^3\chi(k)$ results). The second peak of the inactive chloroplasts, however, seems to lie at approximately the same distance as the third active chloroplast peak and may thus contibute to the active chloroplast's third peak. The third inactive chloroplast peak, when the high noise level of the spectra is considered, seems to be compatible with being a normal second coordination sphere ligand (approximately 3.1Å).

Curve fitting on the inactive chloroplasts was not very successful and, as a consequence, only the T-L one shell fitting results on Fourier isolated R-space peaks are presented in Table 5. The first peak fits show that the

ligands observed are definitely CNO-type, but the value obtained for E_o was 10eV lower than any other CNO ligand studied, which explains the failure of the H-D model fits.[18] This unusual result may imply that the first shell is highly disordered, a hypothesis which could only be explored with signficantly better data. The distance observed is approximately 2.1Å which suggests that it could be contributing to the active chloroplasts' second peak. The second and third peaks in the inactive chloroplast power spectrum could not be separated by the Fourier isolation technique and no acceptable two shell fits were obtained. It was necessary to examine the second peak to see if it might be contributing to the third peak in the active chloroplast power spectrum. A Fourier isolation was performed and the one shell fitting results are included in Table 5. Using the criteria developed to approximately identify the element of a transform peak, the one shell results indicate MnFe based on the qualitative features of the fit. In any case, it has the right distance to be present as part of the active chloroplast's third peak and thus could represent about 1/3 of the magnitude of that peak.

From this analysis it appears that the "tightly bound pool" of Mn did not appear to be affected by removing the "loosely bound pool" of Mn. Thus, if the inactive chloroplast spectrum is multiplied by 1/3 and subtracted from the active chloroplast spectrum, the difference should be a reasonable representation of the EXAFS of the "loosely bound" Mn. The resulting Fourier transforms are presented in Figures 1(g) and 1(h) and Table 1.

(c) Difference Spectrum. Examination of the transforms of this "difference" spectrum created to simulate the EXAFS spectrum for the "loosely bound pool" of Mn shows a marked reduction and slight position shift in the second peak and a 25% reduction in magnitude for the third peak

when compared to the peaks of the active chloroplasts. This is exactly the result expected from comparing the transform peak magnitude of the active and inactive chloroplasts and then forming the difference in R-space.

The curve fits were then performed in a similar manner as before with the same ligand shells as previously identified for the active chloroplasts. The results are listed in Table 6 and the difference spectrum and its best fit are presented in Figure 6.

DISCUSSION

di-μ-oxo Manganese Dimers. Examination of Table 2 reveals a very interesting structural result. The bridging oxygens have the same average distance in Mn(3,4)Bipy and Mn(3,4)Phen while the oxygens Mn(4,4) Phen have the same average distance as the Mn(IV)-oxygen distance in Mn(3,4)Bipy. The Mn-Mn distances for Mn(3,4)Bipy and Mn(4,4)Phen are the same while the Mn(3,4)Phen Mn-Mn distance is 0.02Å shorter. These results thus predict changes in the Mn_1-O-Mn_2 bond angles. Using the average distances from Table 2 and assuming the same ligand distance difference as in Figure 2, the Mn_1-O-Mn_2 angles would be 1) 96.5° for Mn(3,4)Bipy (from the crystal structure[11]), 2) 93.9° for Mn(3,4)Phen, and 3) 97.7° for Mn(4,4)Phen. These are obviously not very large angular changes and therefore would seem to be quite reasonable results. Should the crystal structures of Mn(3,4)Phen and Mn(4,4)Phen be obtained in the future, they will provide very good additional tests of the ability of EXAFS to measure small differences in structurally similar systems.

As mentioned earlier, an explanation for the problem of the missing nitrogen shells in Mn(3,4)Bipy, Mn(3,4)Phen, and Mn(4,4)Phen was developed by examining different simulations of the first coordination sphere of

Mn(3,4)Bipy. The simulations were constructed by using the T-L model values with two oxygen atoms at 1.8Å, two nitrogen atoms at 2.0Å, and two nitrogen atoms at 2.2Å The values of $\tilde{\sigma}_i$ (see equation 3) were then varied to model variable amounts of static and thermal disorder. The simulations had two surprising results. First, if the $\tilde{\sigma}_i$'s were equivalent and small, the result was one nitrogen transform peak, not two as expected, and it was not twice as large as the oxygen peak. One example of this result is given in Figures 1(i) and 1(j) with its numerical analysis tabulated in Table 1. This implies that the nitrogen shells were strongly interfering and while perturbing the oxygen shell transform peak, the strongest effect was upon their own transform peak. Second, if the σ_i's for the nitrogen atoms were significantly more negative than for the oxygen peak (example: $\tilde{\sigma}_N$ = -.005 and $\tilde{\sigma}_0$ = -.001), then the nitrogen atoms badly interfere, resulting in a very small transform peak which would be masked in the model compound transforms by the presence of the Mn peak and a finite noise level. The crystal structure of Mn(3,4)Bipy (Figure 2) shows that the nitrogen atoms are significantly more disordered than are the oxygen atoms[11] so the disappearance of the nitrogen transform peak is not an unphysical result.[20]

A final question which requires consideration concerns the validity the di-μ-oxo manganese dimers as general model compounds for CNO bridged transition metal dimers, since their analyses are cornerstones in the analysis of the active chloroplast "loosely bound pool" of Mn. An extreme change that could be made would be to reduce the Mn atoms[6] and substitute carbon, a much "softer" ligand, for the nitrogen and bridging oxygen ligands. A number of Mn(II) dimer systems with all carbon ligands have been synthesized and studied by Anderson and coworkers.[22] The surprising results are a 2.72A Mn-Mn distance, a distance between the Mn atoms and bridging carbon ligands

of approximately 1.8Å, the same structure as the bridged dimers studied in this paper. Thus, Anderson's compounds and the model systems examined here, which span a large range of Mn oxidation states and two different ligand systems, tend to suggest that the bridged Mn dimer structure is essentially the same irrespective of the Mn oxidation states and the CNO first coordination sphere ligands. Therefore, using the di-μ-oxo dimers as general model compounds seems adequately justified.

Chloroplasts. The chloroplast samples were very dilute in Mn so the resulting XAS spectra were very noisy. Due to the methods of EXAFS analysis this noise level is greatly enhanced at the higher photon energies (higher k-values) where the majority of the multiple distance interference effects would be expected to occur. This makes the analysis difficult and the results less exact for transform peaks which have a very significant part of their k-space data at the higher k-values, e.g., the first two peaks of the active chloroplasts (Figure 4) and the second and third peaks in the inactive chloroplast transforms. The second factor which must be taken into account is the high probability of a significant heterogeneity in "equivalent" local environments present in the model compounds. These two factors result in an assignment of fairly large errors for interatomic distances and only approximate result for the number of backscatters. Thus the approximate distances and the ratios for the number of backscatters is the primary interest as opposed to absolute fitting values.

(a) "Active" Chloroplasts. As mentioned earlier, the key to the identification of the first two peaks in the active chloroplasts power spectrum was a recognition of the similarity between the $k^n\chi(k)$ Fourier transforms of the active chloroplasts and the $k^n\chi(k)$ transforms of some of the simulations of the first two peaks of Mn(3,4)Bipy such as in Figure 1(i)

and 1(j). This observation led to comparing their EXAFS spectra, which were quite similar, and subsequently to performing the T-L fits that are presented in Table 3.

Comparisons of the one shell fits in Table 3 show a completely equivalent behavior with regard to all the fitting parameters (i.e. large positive σ_i's, equivalent changes in distance and E_o, and proportional changes in number of atoms). The second transform peak in either sample produces a strong destructive interference. As k increases, the EXAFS contribution of the second peak rapidly decreases and the EXAFS corresponding to the first peak reappears. The net result of this interference produces a sine wave with frequency corresponding to the distance of the first peak and an amplitude increasing with k (Figure 4). Thus, a T-L model CNO single shell fit compensates for the k dependence of this amplitude function by invoking a large positive disorder parameter (σ_i). This produces a good fit at high k values and a very poor fit at lower k-values.

The two shell T-L fits again show strikingly similar results. As in the one shell fits above, the unusual fitting results arise from having to fit a larger number of real distances with a smaller number of shells. At the present time, as explained in Reference 18(a), fitting more than one shell to one transform peak is unreliable due to a surfeit of fitting parameters. Thus, when three shell fits were attempted on the isolated first two peaks of the active chloroplasts, nonsense was the result, while the fits to the simulations were perfect as expected.

Therefore, just looking at the comparison T-L fits in Table 3, the first peak would be predicted to be CNO with an approximate distance of 1.82Å. The second peak would be CNO with approximately twice the number of atoms of the first peak and results from more than one distinct distance

with a net average of approximately 2.15Å.

The fitting results for all three peaks are tabulated in Table 4 and the noise-filtered $k^3\chi(k)$ spectrum and its best three shell T-L fit is presented in Figure 5. Comparison of the results of the two shell T-L fits on the isolated first two peaks (Table 3) and the oxygen and nitrogen shells of the three shell O-N-Mn T-L fit (Table 4) shows a discrepancy while the N-O-Mn three shell T-L fit (Table 4) agreed with the two shell isolation fitting results (Table 3). Noting that there is little or no visual difference between the two-three shell fits, additional fits were performed with tight constraints on the allowable distances each of the different shells could have. Examining the additional fits shows that the O-N-Mn three shell fit has a local minimum which is equivalent to the two shell fit results of Table 3 and the N-O-Mn fit of Table 4, but there is an interaction between the three shells of the O-N-Mn parameters to produce a slightly better fit, that tabulated in Table 4. This better fit is primarily a compensation by the O-N fitting pair for the T-L model's inability to fit the MeFe shell (third peak) perfectly. It should be noted that additional N-O-Mn fits using starting values similar to the O-N-Mn fit returned to the tabulated result. Thus, this different result is primarily due to the noise level in the original spectrum and a special feature of the choice of the O-N pair, i.e., a model effect. This variable result indicates the range of results which can be obtained when working with disordered systems and having to fit a multicomponent shell with only two model shells. The important three shell results to note are the approximate 2 to 1 ratio for the first CNO shell ligands and the MnFe shell with the distances compatible with the prediction of a bridged structure. The second peak ligands are then the disordered set described above with an average distance

of approxiamtely 2.15Å

(b) "Inactive Chloroplasts. The fitting results on the inactive chloroplast spectrum are discussed in the Results section, and presented in Table 5. The spectrum is noisier than that of the active chloroplasts and the fitting results are less satisfactory but some general conclusions can be drawn about the residual Mn in chloroplasts. First, there may well be more than one site, thus the EXAFS spectrum can be the sum of more than one signal. This can result in very confusing fitting results with only a few model shells as explained previously. Second, the overlap of the second and third power spectrum peaks and the proportionally larger contribution to these peaks from the high k-values have combined to make accurate elemental identification of these shells impossible. However, a tentative analysis suggests that 1) the first coordination sphere is composed of CNO ligands with an average distance of 2.1(1)Å (a reasonable result for a low valent Mn^{+2}); 2) the second coordination sphere is composed of CNO ligands at an average distance of 3.1(1)Å; and 3) some MnFe ligand at a distance of 2.7(1)Å. The MnFe ligand does not seem to be bridged, even though it is at a bridged distance. This suggests that it may result from bridged dimers which have been broken during the Tris treatment but for some reason were not removed during the osmotic shock treatment. In order to fully resolve the tentative nature of these results, significantly better data are required.

(c) Difference Spectrum. As described earlier, the difference spectrum, Figure 6, was created by subtracting from the active chloroplast spectrum the inactive chloroplast spectrum multiplied by one-third. The Fourier transforms are presented in Figure 1(e) and 1(f) and the curve fits are tabulated in Table 6. This difference spectrum has more problems with

noise than the active chloroplast spectrum (as evidenced by the larger least squares fitting errors) but the results are compatible with all the results described above.

The important changes to note between the active chloroplasts and the difference spectrum are 1) the significant decrease in the second peak in the difference spectrum, and 2) the increase in the ratio of the bridging ligands to MnFe ligands from 2 to 1 in the active chloroplasts to 3 to 1 in the difference spectrum.

The decrease in the amplitude of the second peak in the difference Fourier transform is that expected if the second peak of the active chloroplasts arises from more than one Mn site containing a CNO ligand with an approximate distance of 2.1Å. The shortening of the fitted distance tends to suggest that the remaining ligands in the second peak have a little shorter average distance than indicated by the active chloroplast results. It should also be noted that it is possible that the remaining ligands comprising the second peak may not be due to bridged Mn atoms but are due to other Mn atoms that are also released during inactivation. If this is the case, then it will be necessary to study the photosynthetically active Mn in its native environment free of contamination of other Mn atoms that may be present and serve other functions. The possibility of multiple sites would also explain the low absolute number of atoms predicted by the fitting results, but at the present time this should be treated as conjecture until some new evidence indicates otherwise.

The change in the ligand ratio is most likely due to the poorer quality of the difference data, but should not be totally discounted.

CONCLUSION

Three di-μ-oxo Mn dimers were examined using the EXAFS technique. The crystal structure of one of the dimers has been published.[11] Using this published crystal structure, determinations were made concerning certain of the structural parameters for the other two compounds. These results were presented in part (a) of the Discussion section above.

Part of the study of the Mn dimers was concerned with determining why the nitrogen atoms in the first coordination sphere of the dimers did not appear in the EXAFS spectra. A simulation study showed that large disorder in the Mn-N distances was responsible. This simulation study then led to identification of the first two peaks of the active chloroplast Fourier transforms (see Figure 1).

EXAFS studies on the two chloroplast samples and comparison of the chloroplast results with the bridged Mn dimer models has resulted in a prediction for the local structure of the "loosely bound pool" of Mn in chloroplasts which is implicitly related to photosynthetic oxygen evolution. The analysis is compatible with a CNO bridged transition metal dimer (or multimer) similar to the core of the Mn dimer models studied. The chemistry of Mn suggests that oxygen is the most likely bridging ligand but carbon and nitrogen cannot be excluded. The partner transition metal is most likely another Mn, but Fe and Cu cannot be excluded due to their relative abundance in chloroplasts. The remainder of the first coordination ligands is most likely CNO. The distances for the bridging ligands and the other transition metal ligands are quite accurately predicted, but the distance for the other first coordination sphere ligands is poorly defined primarily due to a large spread in the individual ligand distances (see Table 7).

FUTURE WORK

Obvious extensions now in progress are the effects of actinic light, the effects of various redox reagents and known cofactors such as Cl^-. Most important will be the results obtained from a study of the Mn-containing protein whose isolation has been only recently reported by Spector and Winget.[24]

ACKNOWLEDGEMENTS

We wish to thank Dr. T. Wydrzynski, D. Goodin and A. McGuire for helping to characterize the chloroplast samples used in this study. We wish to thank Professors J.F. Dodge and D. Coucouvanis for gifts of samples, T. Walker, N. Kafka and A. Ramponi for help in different phases of the data collection at SSRL, and Professor K. Sauer and Dr. B. McQuillan for useful discussions. M.P.K. was the recipient of a Fellowship from the John Simm Guggenheim Foundation during the course of this work and expresses his thanks to the Foundation and to Dr. M. Gueron, Ecole Polytechnique, Palaiseau, and Dr. Y. Farge, L.U.R.E. University of Paris-South.

This work was performed under the auspicies of the Divisions of Biomedical and Environmental Research and Basic Energy Sciences of the U.S. Department of Energy under Contract No. W-7405-ENG-48 and the National Science Foundation under Grant No. PCM 78-12121. Synchrotron Radiation facilities were provided by the Stanford Synchrotron Radiation Laboratory which is supported by NSF Grant DMR-07692-A02 and the Department of Energy.

Table 1

Fourier Transform (Power Spectra)
Peak Positions and Relative Amplitudes
(E_o = 6565 eV)

Sample (k-space domain)	Peak	$k^0\chi(k)$[a] Effective Distance (Å)	$k^0\chi(k)$[a] Relative Amplitude	$k^3\chi(k)$[a] Effective Distance (Å)	$k^3\chi(k)$[a] Relative Amplitude
Mn(3,4)Bipy (2.5-13.5 Å^{-1})	Oxygen	1.06	1.00	1.37	1.00
	Manganese	1.96	0.53	2.26	0.82
Active Chloroplasts (2.5-12 Å^{-1})	First	1.18	0.48	1.32	0.28
	Second	1.79	0.47	1.68	0.32
	Third	-[c]	-[c]	2.30	0.42
Inactive Chloroplasts (2.5-12 Å^{-1})	First	1.56	1.03	1.57	0.62
	Second	-[c]	-[c]	2.19	0.39
	Third	2.53	0.15	2.64	0.31
Chloroplast[b] Difference (2.5-12 Å^{-1})	First	1.26	0.66	1.31	0.36
	Second	1.81	0.42	1.78	0.17
	Third	-[c]	-[c]	2.29	0.32
Simulated[d] Mn(3,4)Bipy First Shell (2.5-13.5 Å^{-1})	Oxygen	1.20	1.10	1.29	0.54
	Nitrogen	1.68	0.97	1.68	0.63

a) The EXAFS data were multiplied by $k^0 = 1$ and k^3 respectively before Fourier transformation.

b) The EXAFS data were created by Active - 1/3 Inactive. See text.

c) Missing in this Fourier transform. Due to interference effects and noise in the data. Refer to Fig. 1 (a).

d) First shell simulation constructed by using 2 O atoms at 1.8Å, 2N at 2.0 Å and 2 N at 2.2 Å with σ = -.001 for all and the Teo-Lee Model.[9] Amplitude corrected for σ.[18]

Table 2

One Shell Fits to Isolated Peaks
in Mn(3,4)Bipy[a], Mn(3,4)Phen[b] and Mn(4,4)Phen[c] $_{o-1}$
(All fits were performed over a range of k = 4-12A)

Teo-Lee Model

Sample	Fitting[i] error	distance[d]	No. atoms[e]	σ	Eo
Mn(3,4)Bipy					
O	.193	1.812 (19)[g]	1.8	-.0051	6575.0
Mn	.016	2.677 (16)[h]	0.9	-.0068	6548.6
Mn(3,4)Phen					
O	.400	1.811 (19)[g]	2.0	-.0057	6575.9
Mn	.034	2.660 (21)[h]	1.2	-.0105	6544.6
Mn(4,4)Phen					
O	.105	1.778 (16)[g]	1.9	-.0010	6566.1
Mn	.014	2.678 (8)[h]	1.0	-.0069	6546.5

Hodgson-Doniach Model[18,20]

Sample	Fitting error	distance	no. atoms	Eo
Mn(3,4)Bipy				
O	.480[f]	1.790[f]	5.1	6565
Mn	stnd[f]	2.684[f]	1	6565
Mn(3,4)Phen				
O	.650	1.786	6.0	6565
Mn	.060	2.675	1.2	6565
Mn(4,4)Phen				
O	.038	1.786	4.7	6565
Mn	.016	2.686	1.0	6565

a) di-μ-oxo-tetrakis(2,2' bipyridine) dimanganese(III,IV) perchlorate

b) di-μ-oxo-tetrakis(1,10 phenanthroline)dimanganese(III,IV) perchlorate

c) di-μ-oxo-tetrakis(1,10 phenanthroline)dimanganese(IV,IV) perchlorate

d) Phase only fits, amplitude removed from Fourier isolated peak.[18]

e) Corrected for σ.

f) This Mn was used as the backscattering model with the distance correct for Mn_4N.

Table 2 (cont.)

g) Mn(3,4)Bipy average distance = 1.819 Å. Mn(IV)-O distance = 1.784 Å.[11]

h) Mn(3,4)Bipy Mn-Mn distance = 2.716 Å. This distance error of -.039 Å is charateristic of all di-μ-oxo Mn-Mn distances studies (these compounds and Mn_2O_3).[18] Thus Mn(3,4)Phen Mn-Mn = 2.699 Å and Mn(4,4)Phen Mn-Mn = 2.717 A.

i) Average least square error weighted by k^3.

Table 3

Fits on Active Chloroplast Isolated First and Second Shells and Simulated O-N Shell of Mn(3,4)Bipy[a] Using Teo-Lee Model.[d] (σ_{O-1}) (All fits were performed over a range of k = 4-11Å^{-1})

Sample	Fitting atom	Fitting error	distance	no.[b] atoms	σ	ΔE_o[c]
	(a) One shell fits					
Active (1-2)	1) C	.043	1.830 (48)	1.1	+.0105	-17.7
	2) N	.049	1.816 (50)	0.8	+.0116	-14.0
	3) O	.050	1.802 (52)	0.6	+.0127	-10.3
Simulation	1) C	.030	1.813 (80)	1.8	+.0097	-18.0
	2) N	.031	1.800 (80)	1.3	+.0105	-14.0
	3) O	.032	1.786 (80)	1.1	+.0113	-10.3
	(b) Two shell fits					
Active (1-2)	1) O	.0011	1.791	0.9[b]	+.0068	- 8.9
	N		2.193	0.4[b]	-.0104	- 3.0
	2) N	.0012	1.798	0.8	+.0081	-19.4
	O		2.193	0.4	-.0027	1.1
Simulation	1) O	.0002	1.803	1.6[b]	+.0006	- 3.9
	N		2.135	1.0[b]	-.0101	5.3
	2) N	.0014	1.802	1.7	+.0020	-12.6
	O		2.143	1.7	-.0037	12.6

a) Simulation parameters: 2 atoms of O at 1.80 Å, 2 atoms of N at 2.00 Å, 2 atoms of N at 2.20 Å, all σ_i equal to -.001. Amplitudes corrected for σ.[18]

b) Corrected for σ. σ<-.008 for CNO left uncorrected.[18]

c) For active chloroplasts, difference between best fit E_o and 6571.2 eV. For simulated file this is the best fit ΔE_o.

d) See reference 9.

Table 4

Active Chloroplast Three Shell Fits
(All fits were performed over a range of k = 4-11 A^{o-1})

Teo-Lee Model[9]

	Fitting atoms	Fitting error	distance	No. atoms[a]	σ	E_o
1)	O	.0013	1.851	1.4[b]	-.0073	6569.3
	N		2.046	3.3[b]	-.0195	6549.1
	Mn		2.703	0.44	-.0049	6553.4
2)	N	.0036	1.789	1.0	+.0065	6549.2
	O		2.207	0.6	+.0144	6582.0
	Mn		2.688	0.45	-.0040	6550.7

Hodgson-Doniach Model[18,20]

E_o = 6565 eV

	Fitting atoms	Fitting error	distance	No. atoms
1)	O	.0460	1.843	2.72
	N		2.133	1.38
	Mn		2.690	0.55
2)	N	.0490	1.871	1.21
	O		2.135	3.41
	Mn		2.686	0.55

a) Corrected for σ.[18]

b) σ<-.008 for CNO left uncorrected.[18]

Table 5

Inactive Chloroplast Fits Using One Shell
(All fits were performed over a range of k = 4-11 A^{o-1})

Teo-Lee Model[9]

Fit No.	Fitting Atom	Fitting error	distance[a]	no. atoms[b]	σ	E_o
			(a) Isolated First Peak Fits			
1)	C	.157	2.106 (44)	2.5	-.0059	6546.2
2)	N	.124	2.085 (36)	2.1	-.0048	6548.7
3)	O	.094	2.068 (31)	1.8	-.0039	6550.7
			(b) Isolated Second Peak Fits			
1)	C	.0196	2.716 (24)	3.3	+.0008	6548.2
2)	N	.0128	2.696 (18)	2.6	+.0019	6550.0
3)	O	.0079	2.677 (12)	2.1	+.0027	6551.8
4)	S	.0195	2.676 (10)	-1.2	-.0034	6551.3
5)	Mn	.0507	2.674 (8)	0.44	-.0099	6540.7

a) Phase only fits.[18]

b) Corrected for σ. For Sulfur a multiple Mn amplitude correction was used.[18]

Table 6(a)

Fits on Chloroplast Difference
(All fits were performed over a range of k = 4-11 A^{o-1})

Teo Lee-Model[9]

	Fitting atoms	Fitting Error	Distance	Number of Atoms	σ	E_o
			Two Shell Fits			
1)	O	.0344	1.791	0.99[a]	+.0035	6550.0
	Mn		2.711	0.89[c]	-.0279	6557.6
2)	N	.0410	1.806	1.24[a]	+.0025	6546.0
	Mn		2.710	0.87[c]	-.0277	6557.7
			Three Shell Fits			
1)	O	.0063	1.812	0.92[a]	+.0073	6557.4
	N		2.139	0.32[a]	-.0026	6583.0
	Mn		2.694	0.23[c]	-.0225	6554.8
2)	N	.0067	1.809	0.94[a]	+.0101	6548.0
	O		2.077	0.43[b]	-.0563	6583.0
	Mn		2.706	0.29[c]	-.0188	6556.2

a) Corrected for σ.[18]

b) σ<-.008 for CNO shell left uncorrected.[18]

c) σ<-.023 for single Mn shell left uncorrected.[18]
Note that in general the larger σ, the smaller the number of atoms predicted by the fit. If the slope for Mn correction from Reference 18 is used, then all four numbers of Mn atoms are equivalent ± 10%.

Table 6 (b)

Fits on Chloroplast Difference
(All fits 4-11$\AA^{-1}$)

Hodgson-Doniach Model[18,20]

E_o = 6565 eV

	Fitting atoms	Fitting error	Distance	No. atoms
		Two Shell Fits		
1)	O	.243	1.865	0.80
	Mn		2.682	0.39
2)	N	.162	1.848	1.85
	Mn		2.678	0.39
		Three Shell Fits		
1)		.0054	1.854	3.10
	N		2.111	1.13
	Mn		2.677	0.39
2)	N	.0222	1.888	1.51
	O		2.130	2.85
	Mn		2.676	0.38

Table 7

Proposed Ligand Structure of the Photosynthetically Active, "Loosely Bound" Pool of Manganese in Spinach Chloroplasts

Ligand[a]	Average Distance[b]	Number
CNO[c]	1.81 (2)	2-3
CNO	2.15 (5)	2-4
MnFe[c]	2.72 (2)	1

a) CNO = Carbon, Nitrogen, or Oxygen
MnFe = Manganese or Iron or Copper

b) Average results for various fits.

c) Bridged structure with CNO ligands and MnFe ligands in approximately square or trigonal bypyrimid arrangement.

REFERENCES AND NOTED

1. Pirson, A. Z. Botan. 31, 193-267 (1937).

2. Radmer, R.; Cheniae, G. in "Topics in Photosynthesis", Primary Processes of Photosynthesis", Vol. 2, J. Barber, Ed., Elsevier, Amsterdam, 1977, pp. 303-348.

3. Wydrzynski, T., Marks, T., Schmidt, P.G., Govindjee and Gutowsky, H.S. Biochem. 17, 2155 (1978).

4. Blankenship, R.E. and Sauer, K. Biochim. Biophys. Acta 357, 152 (1974).

5. Wydrzynski, T. and Sauer, K. Biochim. Biophys. Acta 589, 56 (1980).

6. Kirby, J.A., Goodin, D., Wydrzynski, T., Robertson, A.S., and Klein, M.P. (submitted).

7. Stern, E.A. Phys. Rev. B., 10, 3027 (1974).

8. Ashley, C.A. and Doniach, S. Phys. Rev. B., 11, 1279 (1975).

9. Teo, B.-K. and Lee, P.A. J. Am. Chem. Soc. 101, 2815 (1979).

10. Cramer, S.P., Hodgson, K.O., Stiefel, E.I., and Newton, W.E. J. Am. Chem. Soc... 100, 2748 (1978).

11. Plaksin, P.M., Stoufer, R.C., Mathew, M., and Palenik, G.J. J. Am. Chem. Soc. 94, 2121 (1972).

12. Cooper, S.R. and Calvin, M. J. Am. Chem. Soc. 99, 6623 (1977).

13. Nyholm, R.S. and Turco, A. Chem. Ind. (London), p. 74 (1960).

14. Kincaid, B.M. PhD Thesis, Stanford University (1975).

15. Hastings, J.B., Kincaid, B.M., and Eisenberger, P. Nuc. Inst. Methods 152, 167 (1978).

16. Jaklevic, J., Kirby, J.A., Klein, M.P., Robertson, A.S., Brown, G.S., and Eisenberger, P. Sol. State Comm. 23 679-682 (1977).

17. Goulding, F.S. and Pehl, R.H. in "Nuclear Spectroscopy and Reactions, Part A" Academic Press, New York, 1974, p. 289.

18. (a) Kirby, J.A., Robertson, A.S. and Klein, M.P. (in preparation).

(b) Kirby, J.A., Ph.D. Thesis, University of California, Berkeley, (1980).

(c) Smith, J.P., Ph.D. Thesis, University of California, Berkeley (1978).

(d) Robertson, A.S., Ph.D. Thesis, University of California (1979).

19. Cramer, S.P., Eccles, T. K., Kutzler, F., Hodgson, K.O., and Doniach, S. J. Am. Chem. Soc. 98, 8059 (1976).

20. Eisenberger, P. and Brown, G.S. Solid State Comm., 29, 481 (1979).

21. (a) Cramer, S.P., Hodgson, K.O., Stiefel, E.I., and Newton, W.E. J.Am. Chem.Soc. 100, 2748 (1978).

(b) Cramer,S.P., Hodgson,K.O., Gillum, W.O., and Mortenson, L.E. J. Am. Chem. Soc. 100, 3398 (1978).

(c) Cramer, S.P., Gillum. W.O., Hodgson, K.O., Mortenson, L.E., Stiefel, E.I., Chisnell, J.R., Brill, W.J., and Shah, V.K. J. Am. Chem. Soc. 100, 3814 (1978).

22. Anderson, R.A., Carmona-Guzman, E., Gibson, J.F., and Wilkinson, G. J.C.S. Dalton, 2204 (1976).

23. The "inactive" Chloroplast sample of this presentation corresponds to the Tris-treated osmoticly shocked" or "shocked" chloroplast sample of Reference 6.

24. Spector, M. and Winget, G.D. Proc. Nat. Acad. Sci. USA 77, 957 (1980).

FIGURE CAPTIONS

Figure 1. Fourier transforms (power spectra) for a number of different samples with results tablulated in Table 1. Spectra (a),(c), (e), (g), and (i) are transforms of $k^0\chi(k)$. Spectra (b), (d), (f), (h), and (j) are transforms of $k^3\chi(k)$. Samples are: (a), (b) Mn(3,4)Bipy; (c), (d) active chloroplasts; (e), (f) inactive chloroplasts; (g), (h) chloroplast difference; and (i), (j) simulated first coordination sphere of Mn(3,4)Bipy (see Table 1).

Figure 2. Structure of Mn(3,4)Bipy as determined by Plaksin,et al., J. Am. Chem. Soc. 94, 2121.[11] (1972).

Figure 3. Fluorescence detected X-ray absorption spectra of the Mn K-edge for (a) "active" chloroplasts and (b) Tris-washed, osmotically shocked or "inactive" chloroplasts.

Figure 4. (a) $k^3\chi(k)$ EXAFS spectrum of isolated first two Fourier transform peaks of the "active" chloroplasts (see Fig. 1) and the best Teo-Lee[9] two shell fit using oxygen and nitrogen ligand atoms. Dotted line is the data and the solid line is the fit.

(b)$k^3\chi(k)$ simulated EXAFS spectrum of oxygen-nitrogen first coordination sphere of Mn(3,4)Bipy corresponding to Figure 1(j), whose parameters are described in Tables 1 and 3 (dotted line). Solid line is best Teo-Lee two shell fit using oxygen and nitrogen ligand atoms.

Figure 5. $k^3\chi(k)$ spectrum for the three main Fourier transform peaks of the "active" chloroplasts (see Fig. 1d(d)) and the best Teo-Lee[9] three shell fit (using oxygen, nitrogen, and manganese ligand atoms, respectively). The dotted line is the data and the solid line is the fit.

Figure 6. $k^3\chi(k)$ difference spectrum of "active" chloroplast spectrum minus "inactive" chloroplast spectrum divided by 3 and the best Teo-Lee[9] three shell fit (using oxygen, nitrogen and manganese, ligand atoms, respectively). The dotted line is the difference and the solid line is the fit.

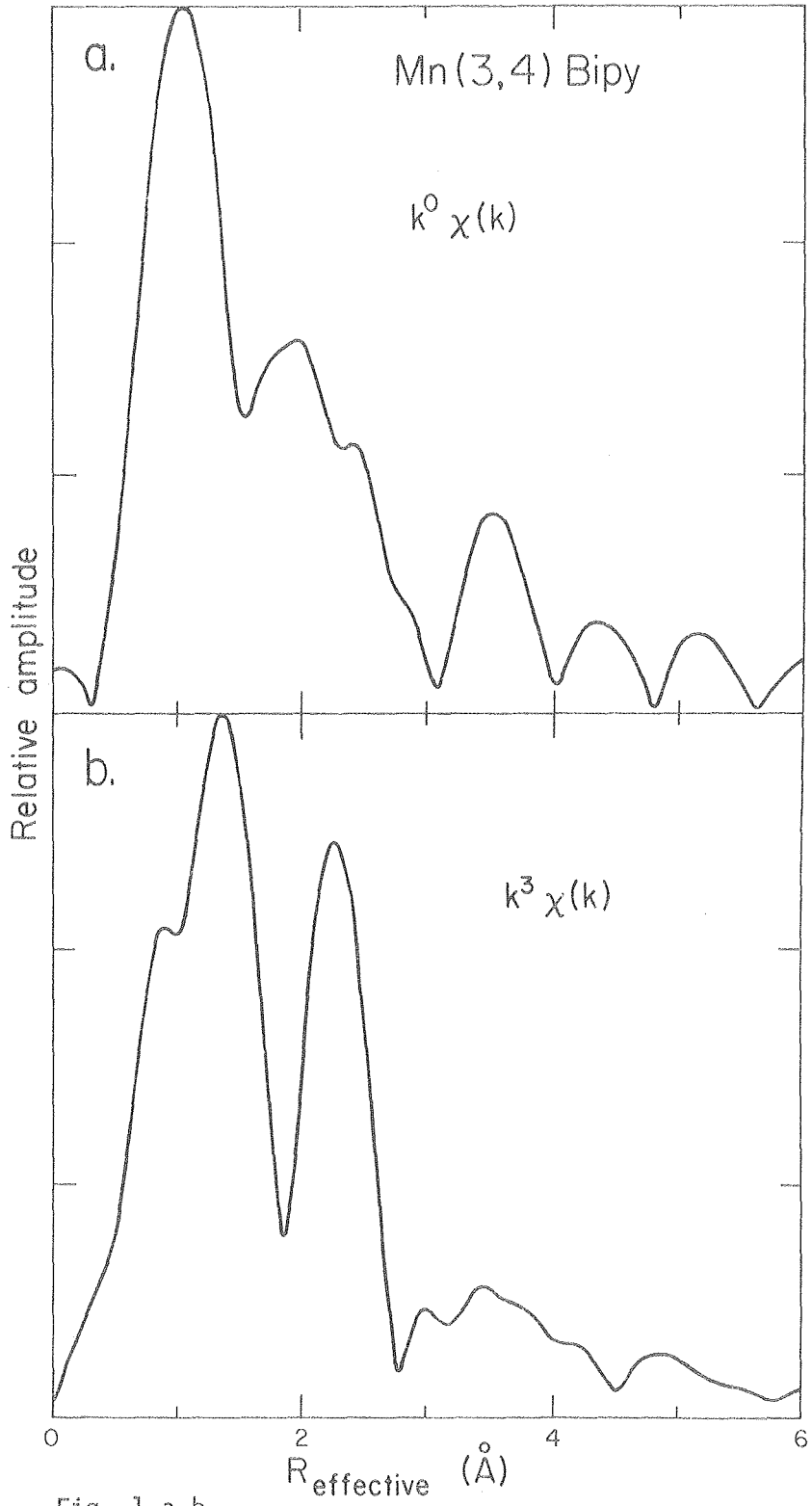
a.
Mn(3,4) Bipy
$k^0 \chi(k)$
b.
$k^3 \chi(k)$
Relative amplitude
0
2
4
6
$R_{effective}$ (Å)

Fig. 1 a,b

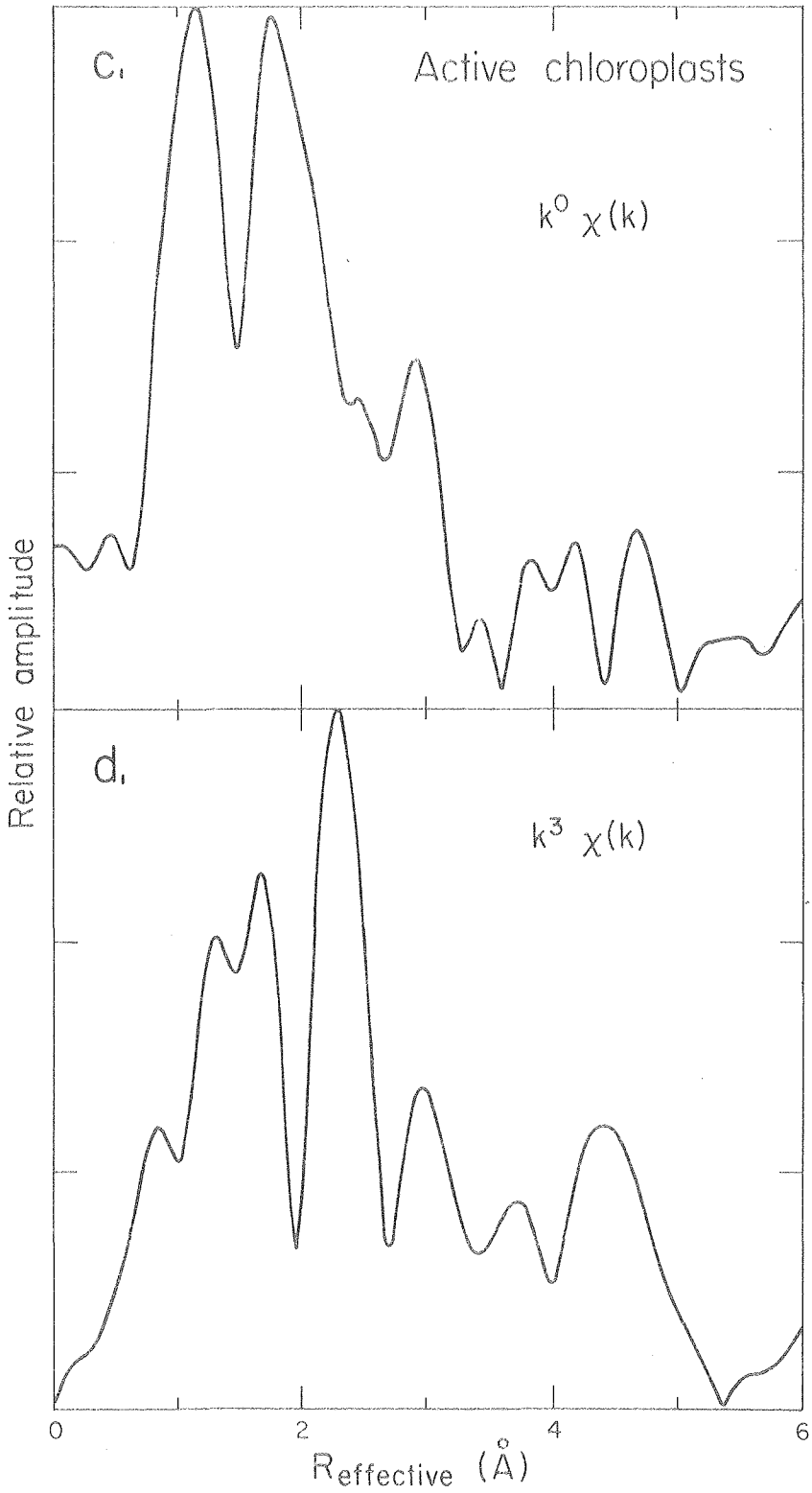

Fig. 1 c,d

XBL 7910-5030

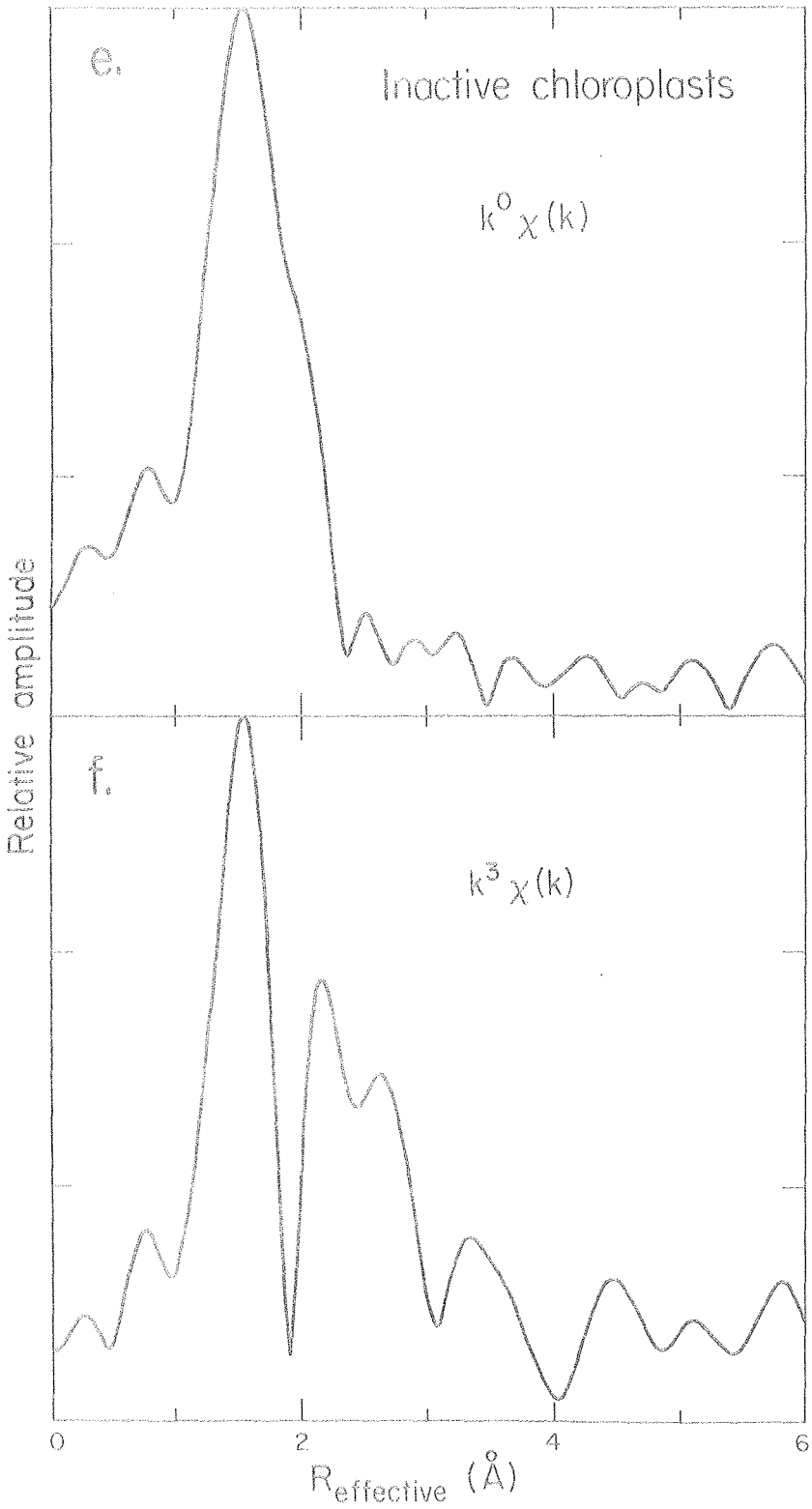

Fig. 1 e,f

XBL 7910-5032

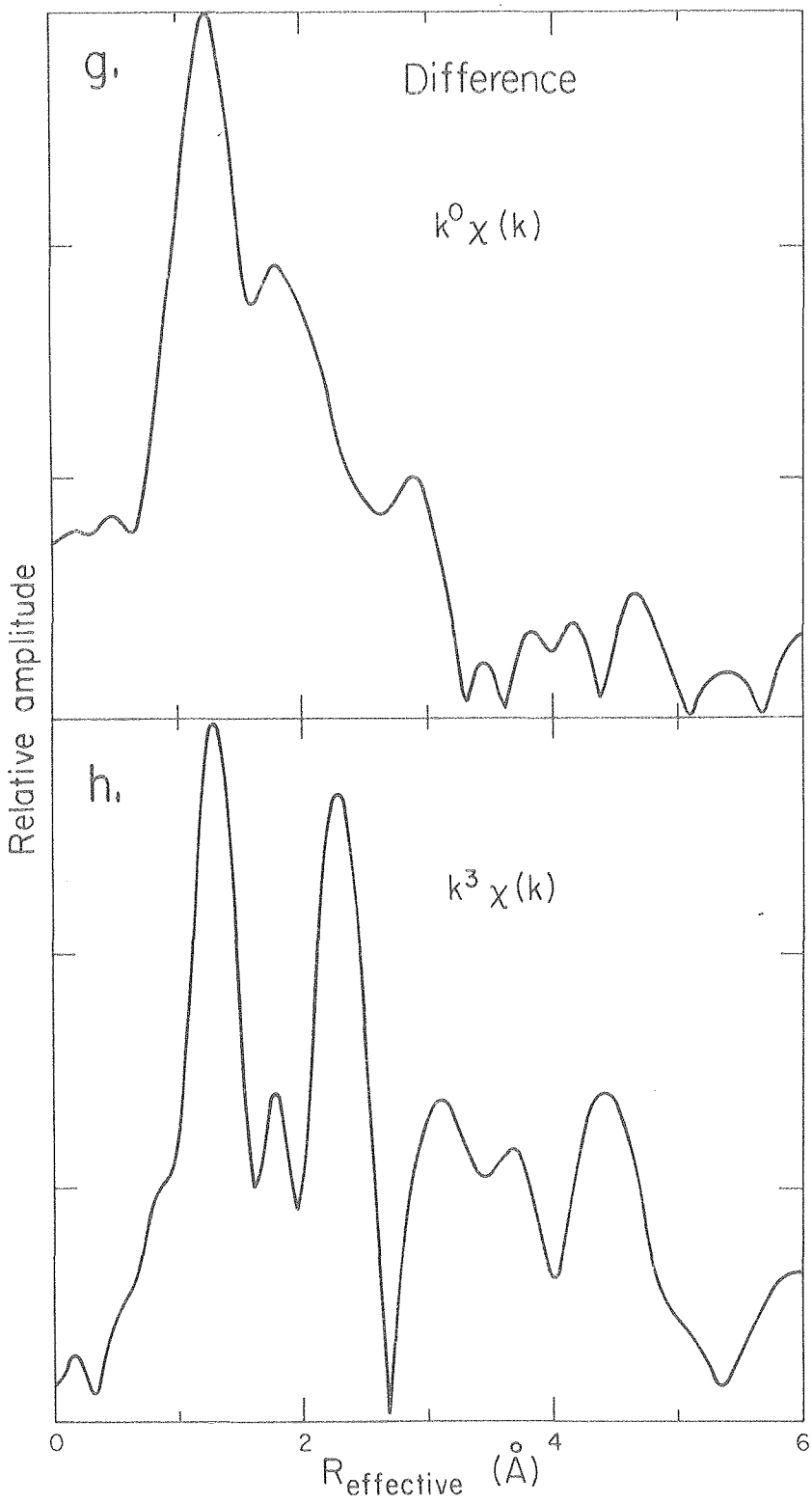

Fig. 1 g,h

XBL 7910-5028

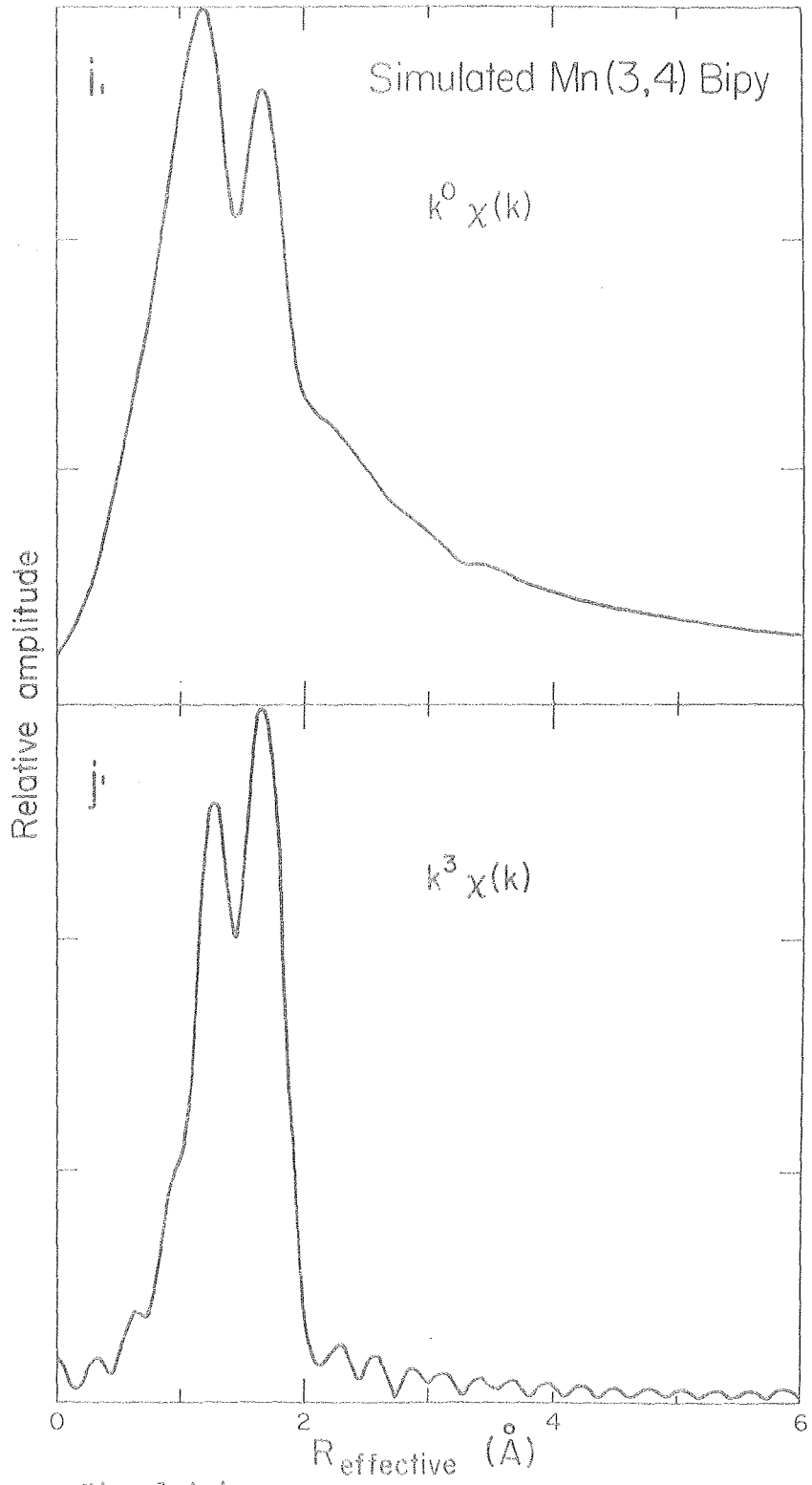
i.
Simulated Mn(3,4) Bipy
$k^0 \chi(k)$
j.
$k^3 \chi(k)$
Relative amplitude
0
2
4
6
$R_{effective}$ (Å)

Fig. 1 i,j

Structure of di-μ-oxo-tetrakis (2,2' bipyridine) dimanganese (III, IV) perchlorate

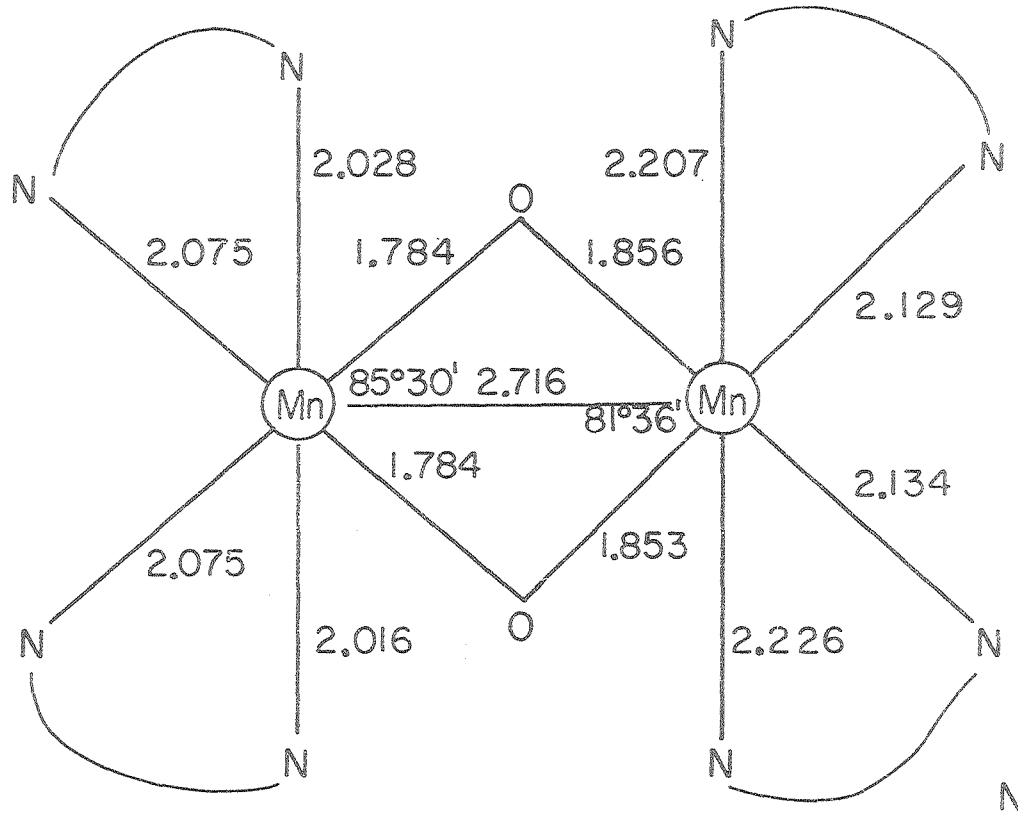

P.M. Plaksin, R.C. Stoufer, M. Mathew, G.J. Palenik, JACS 94 2121 (1972)

Fig. 2

XBL7310-4202

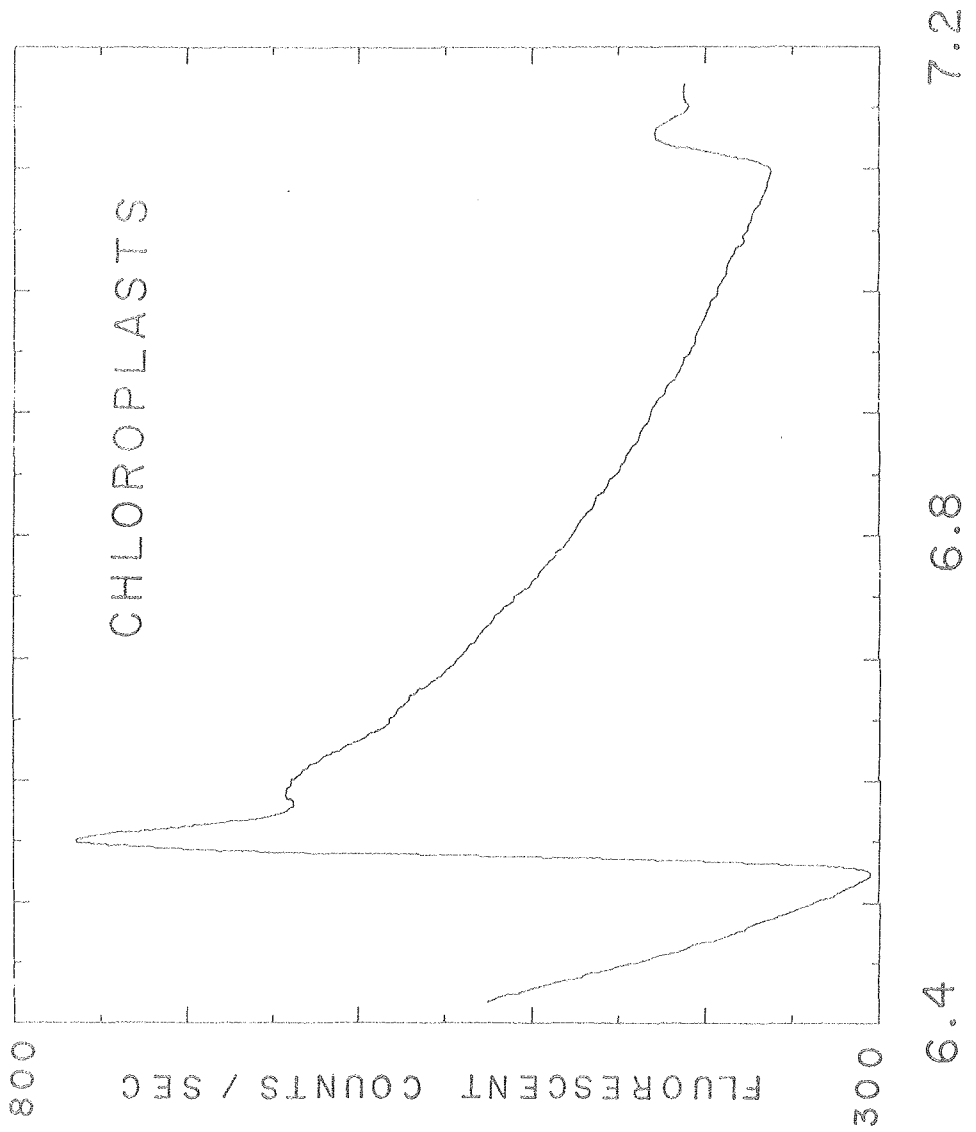

XBL7810-4256

Fig. 3a

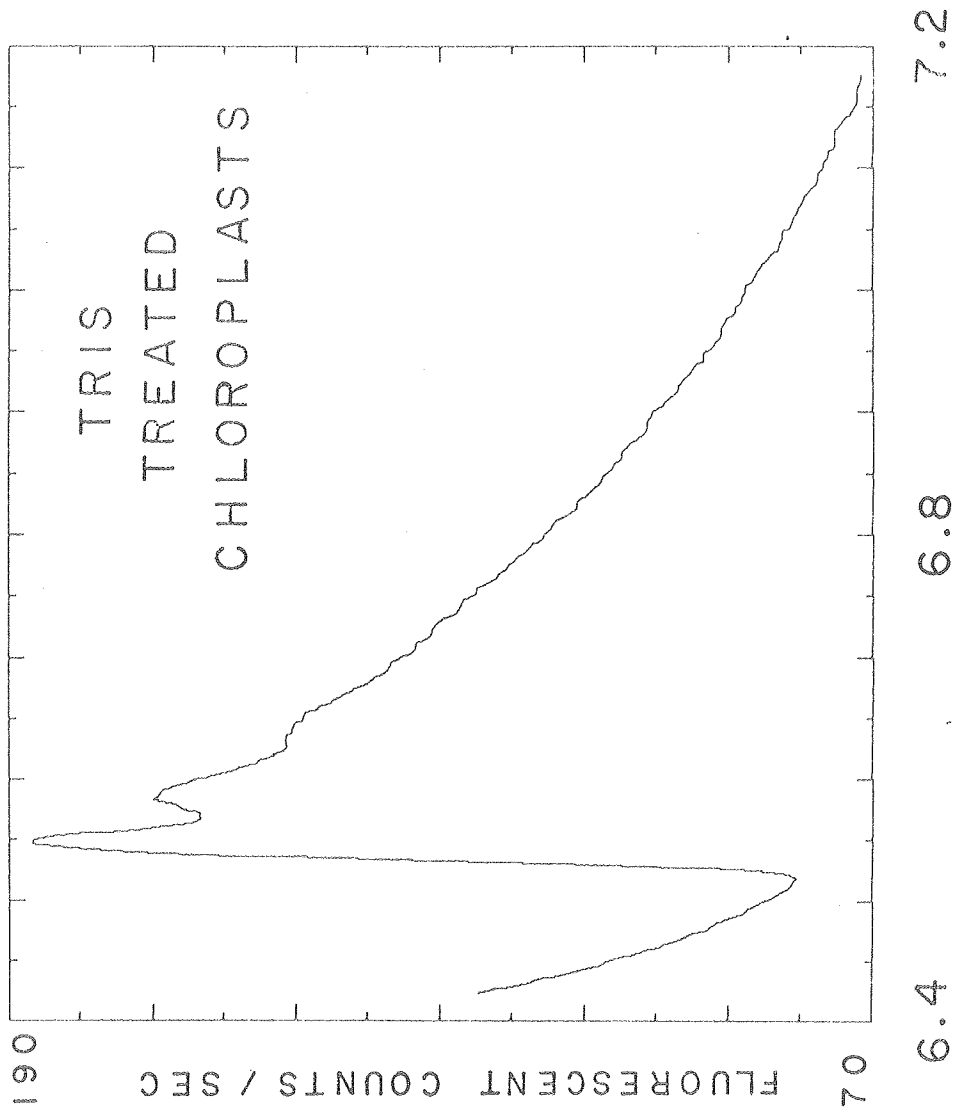

XBL7810-4257

Fig. 3b

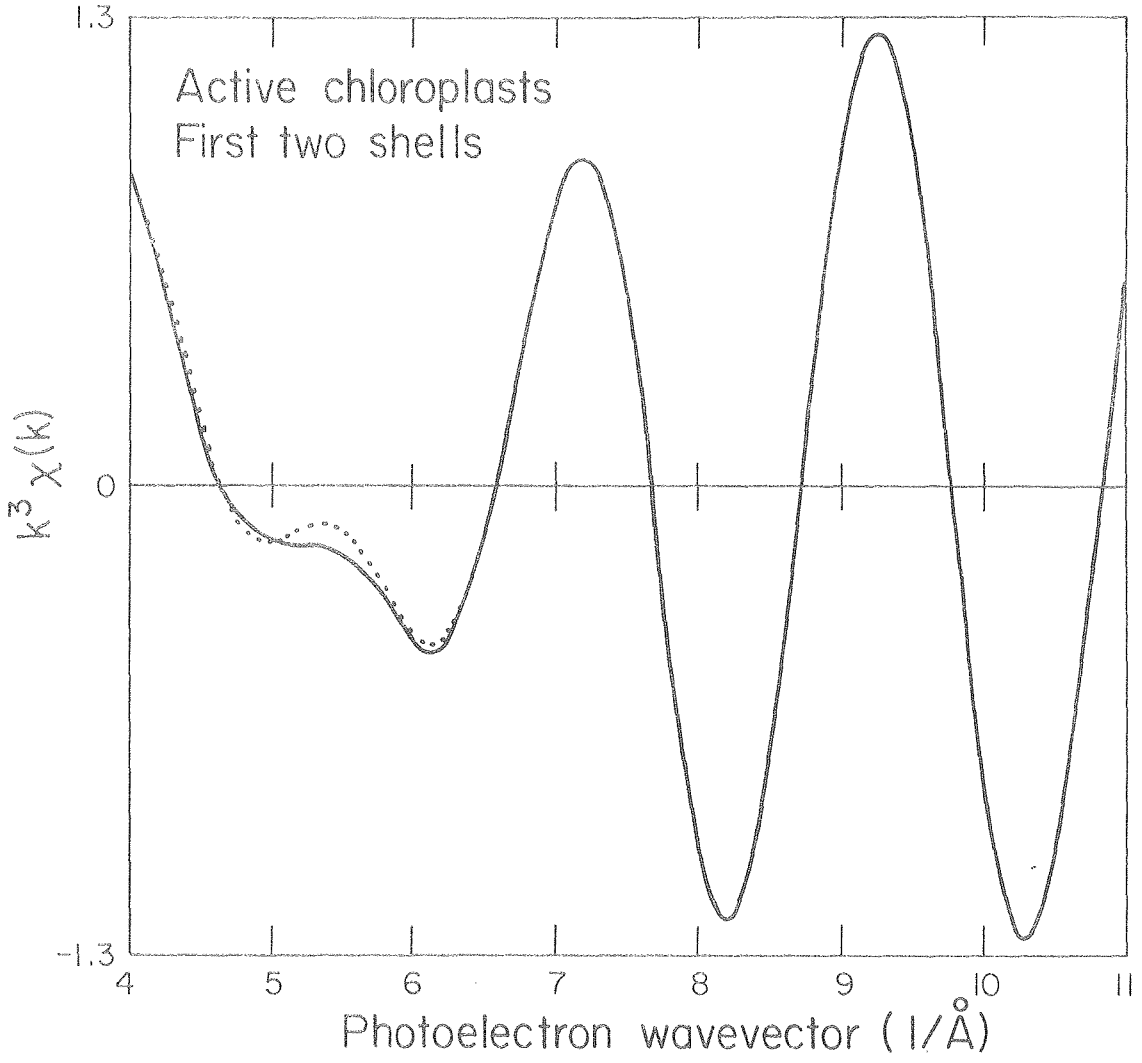

Fig. 4a

XBL 7910-5025

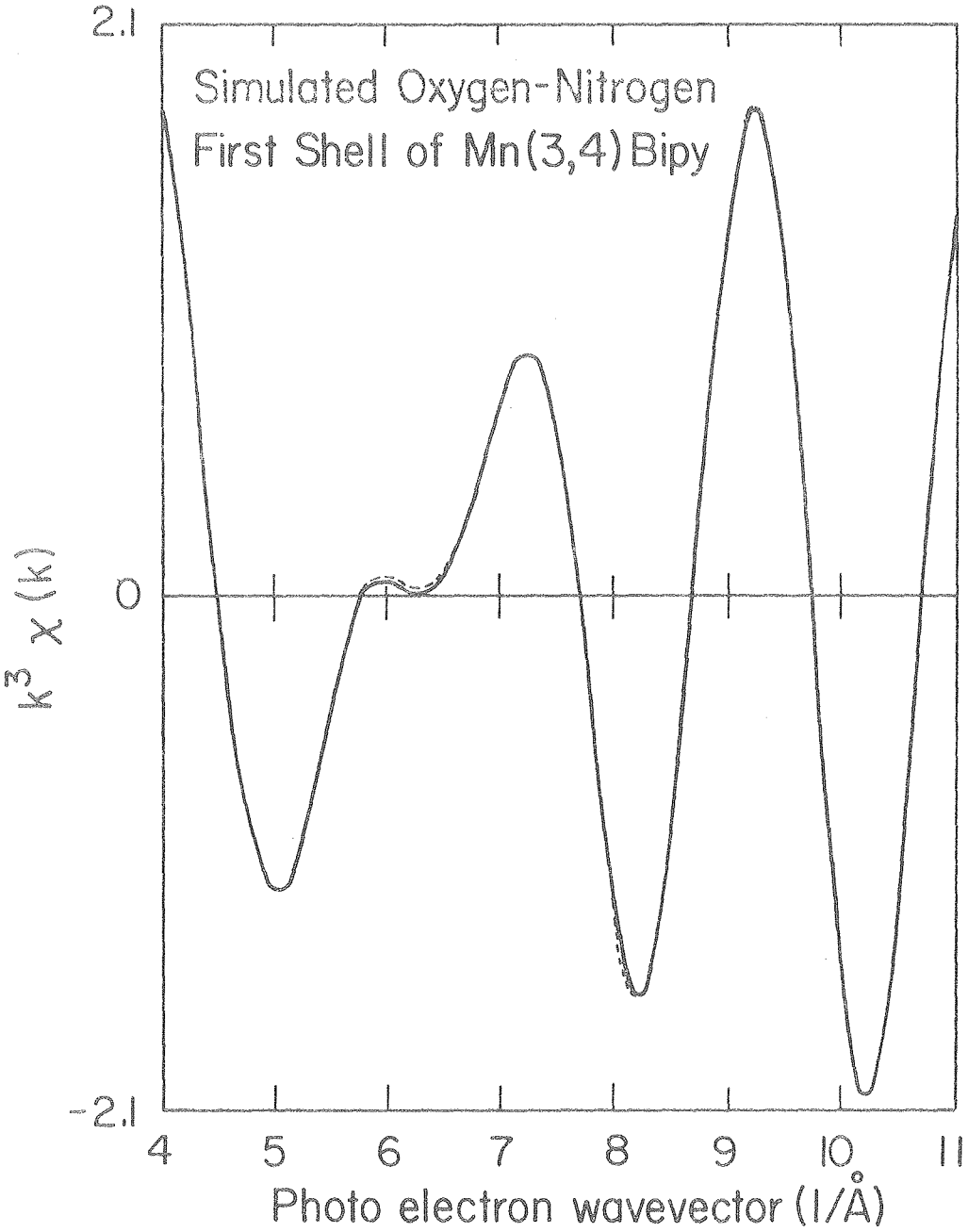

Fig. 4b

XBL 8010-4458

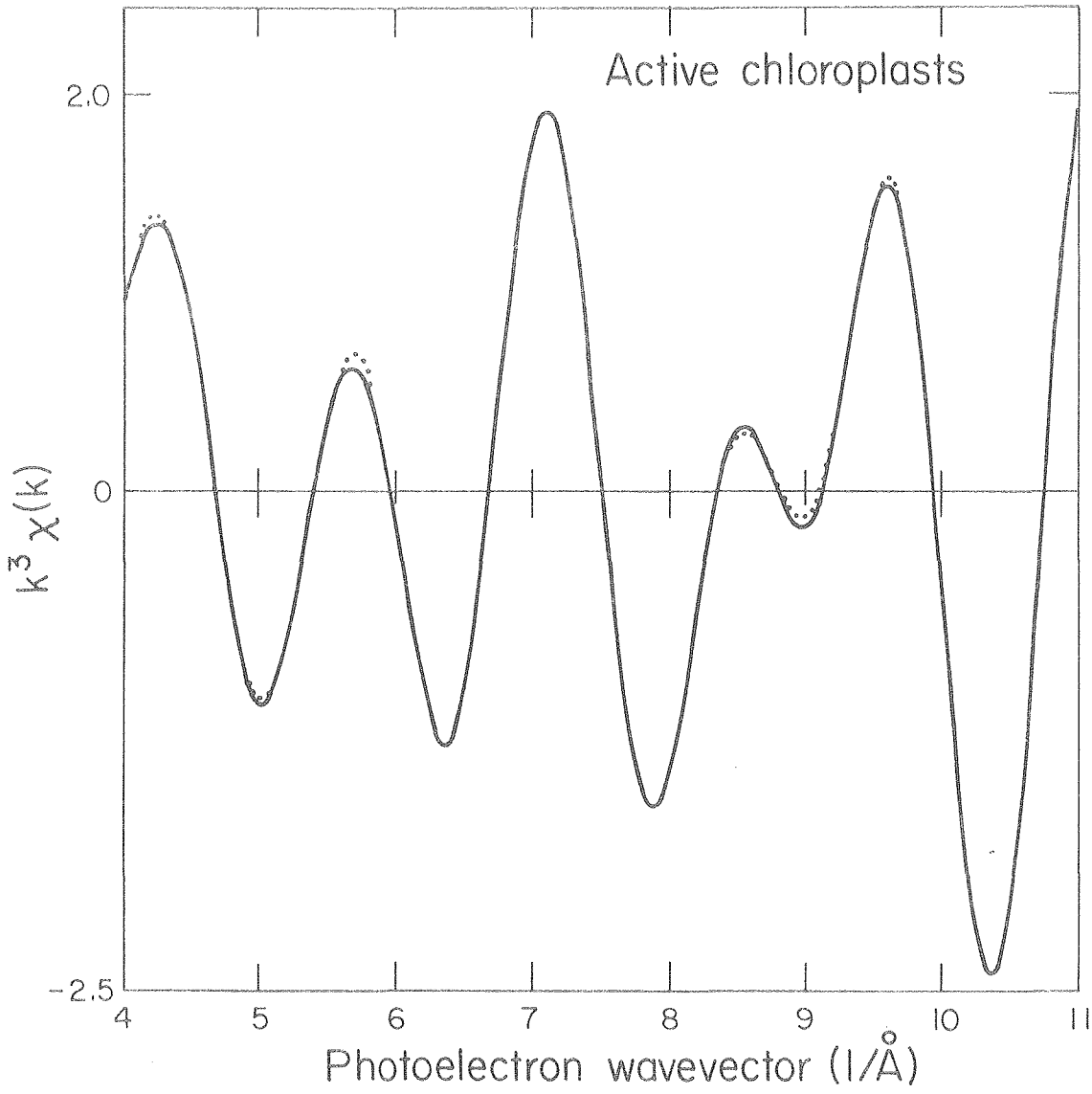

Fig. 5

XBL 7910-5026

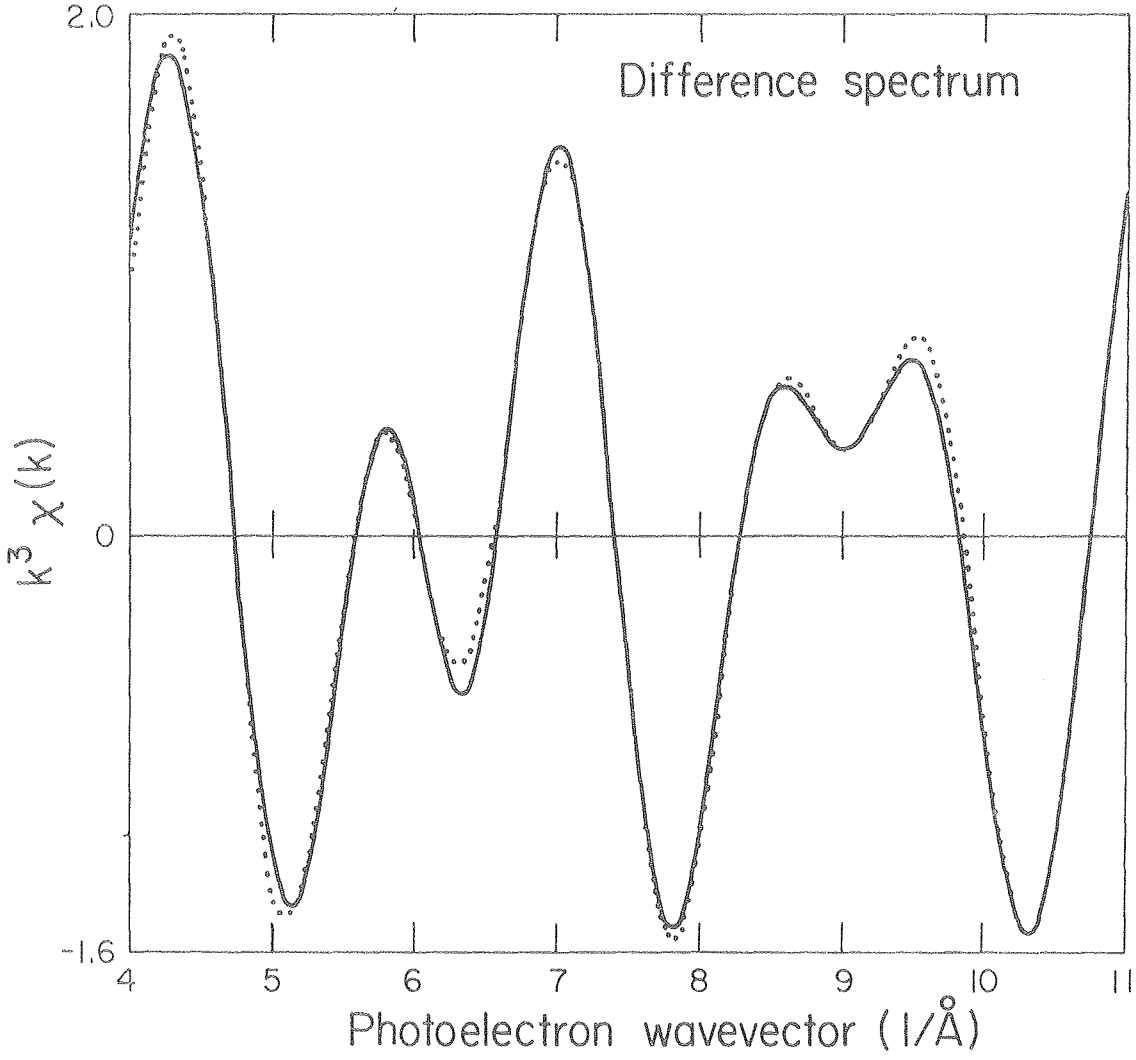

Fig. 6

XBL 7910-5027